

A HIGH-PERFORMANCE MODELING APPROACH OF ARTIFICIAL NEURAL NETWORK AND FINITE ELEMENT ANALYSIS FOR RESIDUAL STRESS PREDICTION OF DIRECT METAL DEPOSITION PROCESS

Farshid Hajializadeh, Ayhan Ince*

Department of Mechanical, Industrial, and Aerospace Engineering, Concordia University, Montreal, Canada

* Email: ayhan.ince@concordia.ca

Abstract— Additive manufacturing (AM) has been extensively attracted attention in both academia and industry. AM is known as progressively deposition of material onto a substrate by implementing a thermal heat source. Although AM provides significant improvements in terms of reducing production cost and time, generation of residual stresses inside the fabricated part, as the result of cyclic heating and cooling, is inevitable. Finite elements (FE) analysis has been used as a tool to predict the residual stress distribution in AM parts. Machine learning methods e.g. artificial neural networks have shown great potential in the determination of the relationship between dependent variable(s) and its variables. An FE-based machine learning framework has been introduced in this context to create a robust modeling tool in the estimation of induced residual stresses in AM parts. In this approach, the results of FE-based models of different geometric structures (L-wall, and box) are considered to train a neural network and the trained network is used to predict the residual stress distribution of larger components. A heat transfer analysis is performed on the large parts and the obtained temperature history is used to predict the residual stress distribution of large parts. The initial results show the great potential of this approach in the prediction of residual stress distribution in AM parts by reducing the computational time considerably.

Keywords: *additive manufacturing, direct metal deposition, residual stress, machine learning, neural network, finite element analysis*

I. INTRODUCTION

Additive manufacturing (AM) process has recently attracted significant interest in both academia and industrial to fabricate complex parts [1]. AM process is regarded as building parts in a sequential and incremental manner by layer-by-layer deposition of material using a thermal heat source [2]. In an AM process, a computer numerical control (CNC) machine is equipped with a thermal source. The geometry of part in the form of a computer aided design (CAD) file is converted into thermal source motions and provided to the CNC machine. Unlike the conventional production methods that required preparing specific tooling and equipment for every single

component, AM shows high potential in developing a feasible and reliable fabrication process of complex parts especially during the design process. AM processes are recognized as efficient and flexible production techniques that facilitates designing procedure of a complex part. The cyclic heating and cooling in the DMD process induces detrimental residual stresses inside the medium [3]. Furthermore, process parameters e.g. laser power, traveling speed of the laser, thickness of the layers, etc. alongside with the material composition and geometrical features of the part have major impacts on the distribution and magnitude of the residual stresses in the DMD process. Therefore, it is essential to evaluate the effect of each parameter on the final characteristics of the DMD products and predict the residual stress distribution to avoid distortions and failure of the products. Finite elements (FE) analysis has shown high potential in prediction of residual stress field and distortion of components built by the DMD process [4]. In order to get reliable results from FE analysis, all applicable process parameters and material properties should be provided in details in FE model. The main drawback of the FE analysis is the high computational time for complex parts. Therefore, several attempts have been made to improve the computational efficiency of FE method by applying different modeling techniques coupled with FE analysis. A mesh coarsening approach was used to enhance the efficiency of the FE analysis of DMD process [5]. The mesh coarsening approach is based on the concept that the areas far from the melt pool in a DMD process can be discretized with coarser mesh grid which results in reducing the total degrees of freedom of the FE model and lowering the computational time. Hajializadeh and Ince [6] developed a FE-based mesh coarsening method for conducting thermomechanical analyses to decrease the computational time of an L-shape part produced by the DMD process.

Recently, researchers applied the concept of machine learning (ML) in field of solid mechanics. Artificial neural networks (ANN) are one of the powerful and commonly used machine learning algorithms in different applications. Koeppel et al. [7] used the FE analysis and experimental data to train ANNs for predicting the stress distribution of specimens made from polylactic acid. The results from ANN model demonstrated good agreement with results of FE model and showed a significant reduction in the computational time.

Liang et al. [8] coupled ML algorithms with computational fluid dynamics (CFD) models for human Aorta to estimate the stress of the Aorta wall of patients. Gulikers [9] developed a computational method by based on ANNs to find an alternative solution for prediction of stress distribution of complex structures. Mortazavi and Ince [10] developed an ANN-based damage model for evaluating the fatigue crack grow rate of several metal alloys both in long and short cracks. It was concluded that the presented model was able to predicting the complex crack growth behavior of both long and short cracks.

In the current study, a novel modeling technique of integrating ANN with FE analysis is presented in order to estimate the residual stress distribution of simple structural parts (an L-shape wall and a rectangular box structures) produced by the DMD process. The training dataset is extracted from results of the FE analysis of 12-layers structural parts. Then, the trained network is used to predict the residual stress distributions of 18 layers parts. The proposed method will be beneficial in terms of providing a efficient and reliable results for studying the effect of process parameters on magnitude and distribution of stress components in AM parts.

II. FINITE ELEMENTS ANALYSIS OF DIRECT METAL DEPOSITION PROCESS

The FE analysis of the DMD process includes the thermal and mechanical analyses. In order to get temperature history, a non-linear transient heat transfer analysis is conducted using the temperature-dependent thermal properties and boundary conditions. Afterward, the element temperature histories are imported to the mechanical analysis to evaluate stress components of the elements. This technique recommended in [6] is called the uncoupled approach. A schematic chart of the uncoupled approach for the FE analysis of the DMD process is demonstrated in Fig.1. By imposing the energy conservation theorem on a medium and using Fourier heat flux constitutive model, the differential equation for calculation of the temperatures can be addressed as [9]:

$$Q(\bar{X}, t) - \rho C_p(T) \frac{dT}{dt} + \nabla \cdot [k(T) \nabla T] = 0 \quad (1)$$

Where \bar{X} is spatial coordinates, t is time, ρ is material density, C_p is specific heat of material, k is conductivity and T is temperature, Q is the body heat source. ABAQUS/STANDARD is used for performing the thermal analysis on the two parts shown in Fig. 2. Each part is an 18-layers component with a thickness of 1 (mm) per layer and with the length (or width) of 15 (mm). UMATHT subroutine is developed for each structure to account for the element activation and also for introducing temperature-dependent material properties to the FE model. Activation of elements and layers were carried out by implementing hybrid element activation technique [6,11-12]. DFLUX subroutine was implemented to provide flexibility in generating desired laser path in conjunction with ABAQUS. A laser heat source with the power of 250 (w), the front semi-axis of 0.5 (mm), and transverse speed of 11.25 (mm/s) was used. Each layer is meshed with 5 elements in the thickness direction with linear brick elements (C3D8T). The material properties of AISI 304L are given in TABLE I. The material density is considered

constant (7800 kgm^{-3}) for AISI 304L for all the thermal analysis.

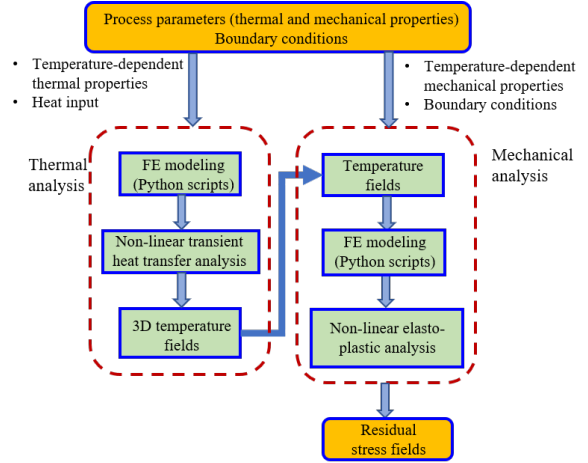


Figure 1. Schematic flow of the uncoupled thermo-mechanical analysis

TABLE I. THERMAL AND MECHANICAL PROPERTIES OF AISI 304L [6]

Temperature (°C)	Specific Heat (J/Kg°C)	Conductivity (J/m °C)	Thermal Expansion ($\times 10^{-5}/^{\circ}\text{C}$)	Yield Stress (MPa)	Young's Modulus (GPa)
20	462	14.6	1.70	319	198.5
100	496	15.1	1.74	279	193
200	512	16.1	1.80	238	185
300	525	17.9	1.86	217	176
400	540	18.0	1.91	198	167
600	577	20.8	1.96	177	159
800	604	23.9	2.02	112	151
1200	676	32.2	2.07	32	60
1300	692	33.7	2.11	19	20
1480	700	120	2.16	8	10

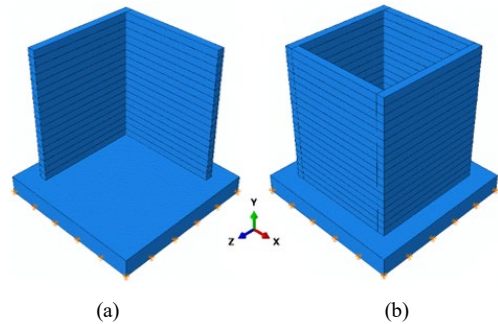


Figure 2. (a) L-shape wall and (b) rectangular wall

The mechanical analysis of DMD is performed upon solving the differential equation obtained from the equilibrium condition expressed in (2) [11,13-15]:

$$\nabla \cdot \sigma + b = 0 \quad (2)$$

in which σ is a 2nd order Cauchy stress tensor, and b is the body force vector. (2) can be solved using the Newton-Raphson iterative scheme by imposing all the boundary conditions and assuming that the small deformation theorem is in place [16]. The nodal displacements and stresses are then

calculated. Similar to thermal analysis, the hybrid element activation scheme is chosen to account for the element activation in the mechanical analysis by developing a UMAT subroutine. To ensure consistency of elements in both analyses, the same mesh size was used in the mechanical analysis as well. 8-node linear brick elements (C3D8) were used to mesh the medium of all the structures. In order to avoid free body motion and also account for substrate effects, the degrees of freedom of the bottom nodes are completely constrained.

III. INTEGRATING ARTIFICIAL NEURAL NETWORKS AND FINITE ELEMENT ANALYSIS

Machine learning is referred to the algorithms that determine the relationships between a set of inputs and output(s) of a system. Artificial neural networks (ANN) are among the well-known algorithms that have shown high capability in finding the criteria of a complex system and have been used in many different fields [17]. Every ANN comprises one input layer, one output layer and one or more hidden layers. All the inputs and outputs are placed in the input and output layer, respectively. In the current study, Keras application programming interface (API) [18] was implemented. Fig. 3 demonstrates the four layers ANN with two hidden layers for configuration of the ANN in the present study. The elements' temperature history and spatial coordinates are set in the input layer and stress values of the elements are put in the output layer. T_1, T_2, \dots, T_f are the temperature history of the elements and $X, Y,$ and Z are the spatial coordinates. Yb is the scaled distance from the substrate. N shows the neuron in every hidden layer and its superscript and subscript show number of the hidden layers and neuron, respectively. i and j show number of neurons in the hidden layers. $S11, S22, S33$ are the stresses in the X, Y (or stacking), and Z directions. $S12, S13,$ and $S23$ are the shear stress components.

The final output of the ANN for every set of input data in each training step (epoch) can be formulated as (3):

$$S_{kl} = \sum_{m=1}^6 S_{m,j} \text{ReLU} \left(\sum_{p=1}^j w_{p,i} \text{ReLU} \left(\sum_{r=1}^i w_{r,n} \overrightarrow{X}_n + b_r \right) + b_p \right) + b_m \quad (3)$$

$$\text{ReLU}(x) = \begin{cases} X & X > 0 \\ 0 & X \leq 0 \end{cases}$$

In order to decide whether a neuron in a layer will be active or silent, *ReLU* (rectified linear unit) that is a nonlinear activation function is used. Initial weights and biases are assigned and the stress components are predicted for each element. Since the predicted stress values differ from the real values, an error function can be considered to evaluate the errors from the real stresses. The mean square error (MSE) was implemented in the current research study. The training of the ANN will perform by conducting minimization on the error function to modify the weights and biases and improve the accuracy of predicted stresses. For training purpose, the gradient descent with back propagation is used [17]. Using Keras API with gradient descent approach using back-propagation ensures the high computational efficiency of the ANN model.

The present study focuses on the integration of ANN with FE analysis for DMD process to boost up efficiency of predicting the residual stresses. Fig. 4 demonstrates a graphical

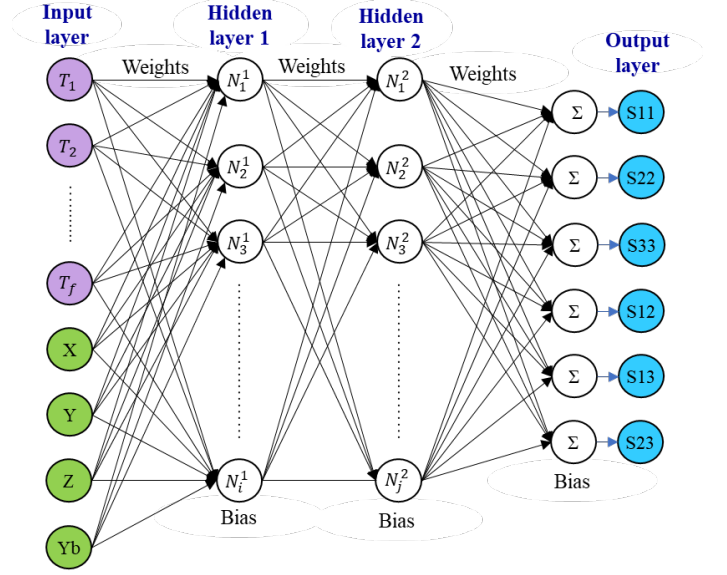


Figure 3. Four layers ANN configuration with two hidden layers

representation of the integrating the ANN with FE analysis to evaluate the stress distribution pattern of parts. The following modeling procedure is performed for both structures, to develop the proposed framework of integrating ANNs and FE:

- Performing detailed thermo-mechanical FE-based modeling of the structural parts;
- Extraction of the training and testing datasets from both 12 and 18-layers structural parts, respectively;
- Configuring features of the ANN based on the size and structure format of dataset obtained from the 12-layers structures;
- Constructing and training the ANN with the training dataset obtained from the 12-layers part;
- Restructuring the input dataset for 18-layers structures to fit the format and size of the trained ANN;
- Feeding the restructured dataset into the trained ANN to predict the stress components and evaluating the prediction error by comparing the predicted ANN results with the FE results.

The training of the ANN is performed by feeding the training dataset extracted from the detailed FE analysis of the 12-layers components. The predictions are made based on the input data and compared with the exact FE results of the 12-layers component for each element. The prediction error is calculated for each epoch and for each element and if they are less than 1%, the training step is completed. Once the network is trained, it can be used for making stress predictions for 18-layers components. Therefore, the input data of the 18-layers structures are fed into the trained ANN to predict stress distribution of 18-layers structures and investigate the accuracy

and capability of the proposed novel ANN-FE framework. However, an additional step may be required before feeding the input data extracted from 18-layers structures into the ANN.

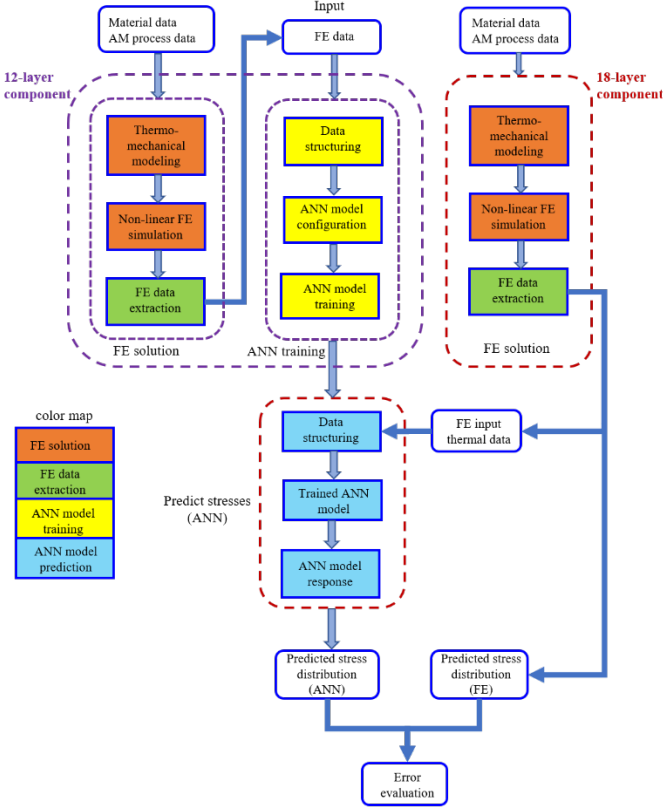


Figure 4. Schematic algorithm of the novel approach of integrating ANN and FE analysis

Elements in the lower layers present a very long and repetitive sequence of lumped temperature histories. Therefore, by removing the undesired and constant temperature sequence for those elements, the testing input vector for every element becomes compatible with the trained network. Finally, the stress components of all elements are predicted for the 18-layers structures.

IV. RESULTS AND DISCUSSION

The error scatter of the predicted results of 18-layers structures are calculated to show the error of the prediction for every element in a 3D contour using (4). Moreover, the histogram analysis is performed on the stress prediction errors to better represent the error dispersion of the proposed novel ANN-FE framework and emphasize on the capabilities of the method.

$$Error_{\sigma} = \left| \frac{\sigma_{prediction} - \sigma_{FE}}{\sigma_{prediction}} \right| \quad (4)$$

A. 18-layers L-wall

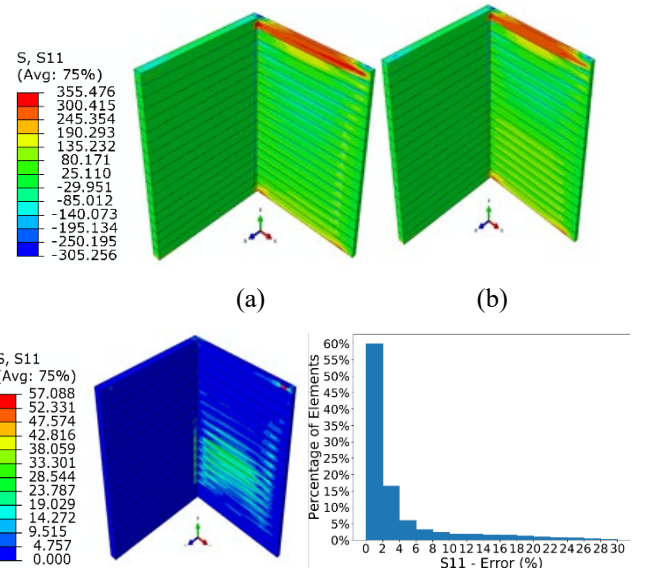
Fig. 5 shows distribution of S11 stress along the X-axis of the 18-layers L-wall. It is concluded that the stress distribution

of the L-wall structure obtained from the integrated ANN-FE approach is consistent with results of the detailed FE analysis by comparing Fig. 5(a) and (b). Furthermore, the predicted stresses in the area with the highest tensile stresses are accurate and are in good agreement with the FE results. The regions shown with blue color in Fig. 5 (c) demonstrate the area with an error of less than 5%. It is noticed that a few elements on the top layer show a high error. The area illustrated by light green and light blue colors are related to the S11 ranges of -50 to 50 MPa that is considered as the low-stress state and can be neglected. Furthermore, by performing the histogram analysis, the percentage of the elements based on the error ranges can be specified. Only 6% of the elements represent error higher than 15%, approximately.

Distribution of the S22 for the 18-layers L-wall is shown in Fig. 6. According to Fig.6 (a) and (b), it is noted that the stress distribution in the stacking direction is consistent for both figures. The novel approach of integrated ANN-FE shows its high capabilities by capturing very smooth transition of stress from tensile to compressive in the middle part of both sides of the L-wall structure. Fig. 6(c) shows the prediction error of the integrated ANN-FE approach for S22 stress. The light green corresponds to the highest prediction error of 10% on the right-hand side of the structure. By performing the histogram analysis on the error scatter data for the right-hand side of the structure, it can be shown that about 2.5% of the elements demonstrate error greater than 10%.

B. 18-layers rectangular box

The distribution of S11 for the 18-layers rectangular box structure is shown in Fig. 7. According to Fig. 7(a) and (b), it is evident that the predicted S11 from the novel integrated ANN-FE method are in good agreement with the result of the detailed FE analysis. The area with high tensile stresses (mid-top layer) and high compressive stresses (the two ends of the top layer) are well-captured by the ANN-FE and it shows the high capability of the novel integrated ANN-FE approach. Error scatter in form of contour is calculated and shown in Fig. 7(c). Majority of the elements represented by blue color show the



(c) (d)

Figure 5. S11 distribution of 18-layers L-wall (in MPa) (a) FE analysis (b) integrated ANN-FE (c) error value (%) (d) error histogram

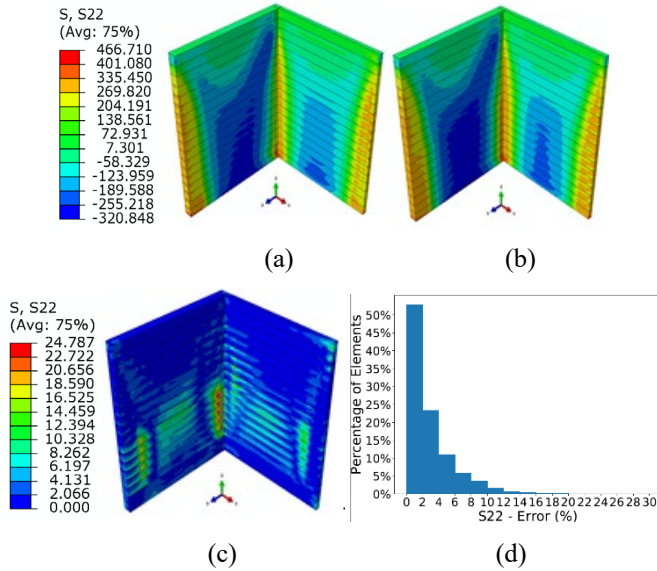


Figure 6. S22 distribution of 18-layers L-wall (in MPa) (a) FE analysis (b) ANN prediction (c) error value (%) (d) error histogram

prediction error less than 3.5%. A very limited number of elements demonstrate very high error values (42%) and can be neglected. The middle part of the component shows an area with the error value of approximately 20%. However, considering that the S11 stress values in those regions are not high, the prediction error is not considered as high. The histogram analysis is assessed for the error scatter data to show the capability of the method for predicting the residual stress of 18-layers box. It is noted that approximately 5% of the elements demonstrate the error values higher than 15%. Therefore, the area with green color with high error percentage will not impose significant problem in implementing the ANN-FE approach.

The distribution of S22 stress for the 18-layers rectangular box is shown in Fig. 8. According to Fig. 8 (a) and (b), it is evident that the stress distribution pattern is in good agreement and the stress profile predicted by the novel ANN-FE approach follows the stress profile in the detailed FE results. The high capability of the ANN-FE is proven by considering its ability of predicting high tensile and compressive stresses and the smooth transition between them. High compressive stresses are well-captured in the inner side of the box based on implementing ANN-FE approach. Very high portion of the elements with less than 4% error are shown with blue color in the error contour demonstrated in Fig. 8 (c). Finally, the histogram analysis is performed on the error scatter data to categorize them based on the error range and portion of the elements. Based on Fig. 8 (c), only 5% of the elements have the stress prediction error higher than 15%. Considering that the very low portion of the elements of 18-layers box structure represent higher than 15% error, it is concluded that the integrated ANN-FE approach is a suitable candidate for stress analysis of DMD components.

TABLE II summarizes the computational times of the FE-based models and the ANN-FE models for 18-layers L-wall and rectangular box. According to TABLE II, it is evident that

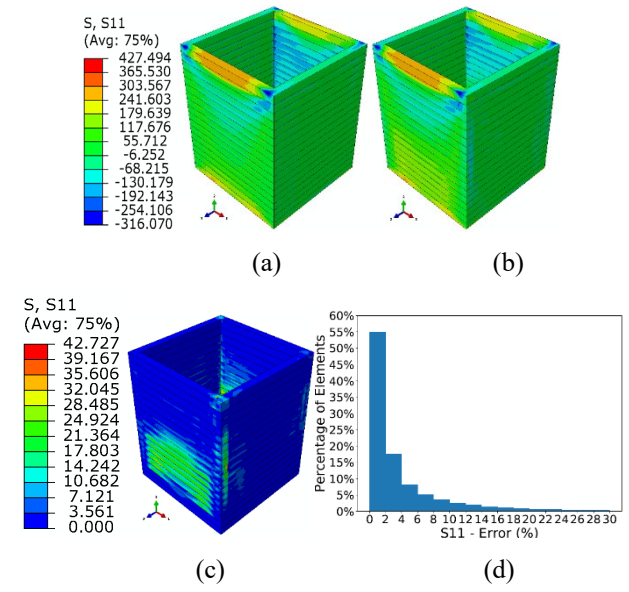


Figure 7. S11 distribution of 18-layers L-wall (in MPa) (a) FE analysis (b) integrated ANN-FE (c) error value (%) (d) error histogram

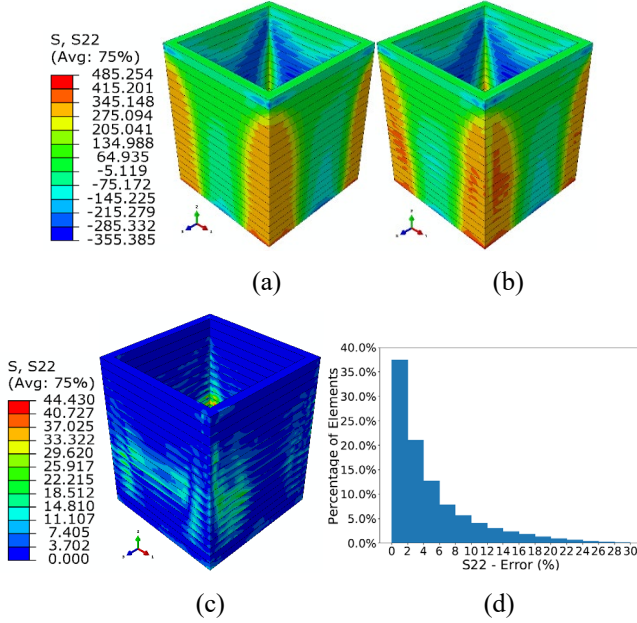


Figure 8. S22 distribution of 18-layers L-wall (in MPa) (a) FE analysis (b) ANN prediction (c) error value (%) (d) error histogram

the computational time of the stress assessment using the novel ANN-FE approach has been improved significantly comparing to the FE analysis. For the 18-layers L-wall, the improvement in the computational time is almost 5.3 times and for the 18-layers rectangular box it is almost 6.1 times. It should be noticed that the training time of the ANN has significant impact in the total time of stress assessment using ANN-FE approach. However, the network is trained only once and it can be used for further stress assessments if different temperature histories

are applied. It is well-suited for investigation of the effect of every process parameter. Therefore, the computational time for the subsequent stress assessments will be significantly lower because the network is not to be trained again.

TABLE II. COMPARISON OF COMPUTATIONAL TIME BETWEEN FE-BASED MODEL AND ANN-FE MODEL

Structure		18-layers L-wall	18-layers rectangular box
Run time	FE analysis	69 h	128 h
	Integrated ANN-FE	12 h	20 h

V. CONCLUSION

In the present study, a new technique of integrating ANN with FE analysis is proposed and developed to improve the computational time for stress assessment of parts fabricated by DMD process. The ANN-FE framework is applied on two simple structures (L-wall and rectangular box) to investigate its capability of being used for modeling the thermomechanical phenomena in DMD process. At first, the dataset for training the ANN is extracted from the results of the detailed FE analysis of 12-layers structures. The ANN is trained based on the training dataset and used for making stress predictions of 18-layers structures. Finally, the error scatter is formed for every component by comparing the results of the novel integrated ANN-FE approach with the exact results of the FE analysis for 18-layers structures. The key factors and outcomes of the present research study are listed in the following:

- A very good agreement was found between the results of the integrated ANN-FE approach and FE analysis for both 18-layers L-wall and rectangular box.
- The ANN algorithms show their promising capability of being employed in the field of studying complex material deformation behavior and for prediction and evaluation of residual stresses in the DMD process.
- The results of employing the ANN-FE showed that it is well-suited for complex geometries than simple ones.
- Majority of the elements in both structures showed error percentages less than 10%.
- By the integrated ANN-FE approach, the computational time for residual stress prediction has been improved significantly; reduction in the computational time by a factor of 5.3 and 6.1 for 18-layers L-shape rectangular box, respectively.

ACKNOWLEDGMENT

The authors would like to acknowledge the financial support of Natural Sciences and Engineering Research Council of Canada (NSERC) (DGECR-2018-00232).

REFERENCES

- [1] J. Ning, E. Mirkoohi, Y. Dong, D. E. Sievers, H. Garmestani, and S. Y. Liang, "Analytical modeling of 3D temperature distribution in selective laser melting of Ti-6Al-4V considering part boundary conditions," *Journal of Manufacturing Processes*, vol. 44, pp. 319-326, 2019.
- [2] L. E. Murr et al., "Metal fabrication by additive manufacturing using laser and electron beam melting technologies," *Journal of Materials Science & Technology*, vol. 28, no. 1, pp. 1-14, 2012.
- [3] X. Liang, L. Cheng, Q. Chen, Q. Yang, and A. C. To, "A modified method for estimating inherent strains from detailed process simulation for fast residual distortion prediction of single-walled structures fabricated by directed energy deposition," *Additive Manufacturing*, vol. 23, pp. 471-486, 2018.
- [4] T. Mukherjee, W. Zhang, and T. DebRoy, "An improved prediction of residual stresses and distortion in additive manufacturing," *Computational Materials Science*, vol. 126, pp. 360-372, 2017.
- [5] S. Jayanath and A. Achuthan, "A Computationally Efficient Finite Element Framework to Simulate Additive Manufacturing Processes," *Journal of Manufacturing Science and Engineering*, vol. 140, no. 4, p. 041009, 2018.
- [6] F. Hajjalizadeh and A. Ince, "Finite Element based Numerical Modeling Framework for Additive Manufacturing Process," *Mat Design Process Comm.*, pp. 1-7, 2019.
- [7] A. Koeppe, C. A. H. Padilla, M. Voshage, J. H. Schleifenbaum, and B. Markert, "Efficient numerical modeling of 3D-printed lattice-cell structures using neural networks," *Manufacturing Letters*, vol. 15, pp. 147-150, 2018.
- [8] L. Liang, M. Liu, C. Martin, and W. Sun, "A deep learning approach to estimate stress distribution: a fast and accurate surrogate of finite-element analysis," *Journal of The Royal Society Interface*, vol. 15, no. 138, p. 20170844, 2018.
- [9] T. Gulikers, "An Integrated Machine Learning and Finite Element Analysis Framework, Applied to Composite Substructures including Damage," 2018.
- [10] S. Mortazavi and A. Ince, "An artificial neural network modeling approach for short and long fatigue crack propagation," *Computational Materials Science*, vol. 185, p. 109962, 2020.
- [11] E. R. Denlinger, J. C. Heigel, and P. Michaleris, "Residual stress and distortion modeling of electron beam direct manufacturing Ti-6Al-4V," *Proceedings of the Institution of Mechanical Engineers, Part B: Journal of Engineering Manufacture*, vol. 229, no. 10, pp. 1803-1813, 2015.
- [12] F. Hajjalizadeh and A. Ince, "Short review on modeling approaches for metal additive manufacturing process," *Material Design & Processing Communications*, vol. 2, no. 2, p. e56, 2020.
- [13] Q. Yang, P. Zhang, L. Cheng, Z. Min, M. Chyu, and A. C. To, "Finite element modeling and validation of thermomechanical behavior of Ti-6Al-4V in directed energy deposition additive manufacturing," *Additive Manufacturing*, vol. 12, pp. 169-177, 2016.
- [14] Y. Yang, M. Jamshidinia, P. Boulware, and S. Kelly, "Prediction of microstructure, residual stress, and deformation in laser powder bed fusion process," *Computational Mechanics*, pp. 1-17, 2018.
- [15] E. R. Denlinger, J. Irwin, and P. Michaleris, "Thermomechanical modeling of additive manufacturing large parts," *Journal of Manufacturing Science and Engineering*, vol. 136, no. 6, p. 061007, 2014.
- [16] R. I. Borja, *Plasticity: modeling & computation*. Springer Science & Business Media, 2013.
- [17] B. Yegnanarayana, *Artificial neural networks*. PHI Learning Pvt. Ltd., 2009.
- [18] N. Ketkar and E. Santana, *Deep Learning with Python*. Springer, 2017.